On Fundamental Limitations for Rudder Roll Stabilization of Ships

Graham C. Goodwin, Tristan Pérez, Maria Serón and Ching Yaw Tzeng

Dept. of Electrical and Computer Engineering
The University *of* Newcastle, Callaghan, NSW 2308, Australia

Abstract

The main purpose of the rudder in ships is course keeping. However, the rudder can also be used, in some cases, to reject undesirable wave produced rolling motion. From a fundamental point of view, the main issues associated with this problem are the presence of a non minimum phase zero and the single input two output nature of the system. In this paper, the limitations imposed on the achievable closed loop performance due to these issues are analyzed. This gives a deeper understanding of the problem and leads to conclusions regarding the inherent design trade-offs which hold regardless of the control strategy used.

1 Introduction

Rudder Roll Stabilization (RRS) is an attractive method for reducing ship rolling motion produced by waves. By so doing, cargo damage is prevented, while crew efficiency and passenger comfort are improved. RRS uses the capacity of the rudder to produce roll motion apart from its normal course keeping function.

Using the rudder for simultaneous course keeping and roll reduction raises non trivial issues since there is only one actuator available to achieve two objectives. Therefore, trade-offs are expected to limit the achievable closed loop performance.

Several control schemes have been proposed in the literature to address RRS. These schemes use different approaches, *e.g.*, Quantitative Feedback Theory [4], LQR [2], and Model Predictive Control [5]. However todate, a little has been said about the fundamental limitations imposed on the closed loop performance by the single input two output (SITO) nature of the problem. The system has also a non minimum phase (NMP) zero, and it is known that this usually limits the achievable performance.

The characterization of the best achievable performance in terms of the intrinsic dynamics and structure of the system reveals what is and, conversely, what is not achievable prior to applying any specific technique for solving the control problem. This leads to key conclusions about the trade-offs inherent in the achievable closed loop performance that hold irrespective of the control strategy being used.

The layout of the paper is as follows. In section 2, a brief review of the Rudder to Roll and Yaw interaction mechanism is given as well as a model of the associated dynamics. In section 3, the objectives of RRS are presented, and a feedback structure is given to address the problem. In section 4, the presence of the NMP zero associated with the Roll dynamics is analyzed, and expressions, based on Poisson integrals, for evaluating the sensitivity trade-off are given. In section 5, an optimization approach is used to analyze the trade-off between keeping the roll angle small whilst maintaining the heading of the ship in a given sea condition. Conclusions are drawn in section 6.

2 Rudder to Roll and Yaw Dynamics

When the rudder is moved away from the central position, a lift force, called *rudder force*, appears on the rudder. Since the size of the rudder is relatively small, the rudder force is small. However, the roll moment it produces is large since the rudder is located at the bottom of the hull. This moment produces rolling motion. At the same time, the rudder force also produces a yaw moment. This moment is also small but once the ship has a small turning deviation, there exists an angle of attack between the hull and the water flow which produces a lift force acting on the hull. This force, called *the hull hydrodynamic force*, supplies the centripetal force necessary for turning motion, and also produces a roll moment as the hull hydrodynamic force acts halfway along the draft. This moment is opposite and larger than the one produced by the rudder, and gives rise to the NMP behaviour associated with the rudder-roll dynamics. Another relevant characteristic of this system is that the rudder-yaw dynamics contain an integrator.

To describe the rudder roll and yaw generated motion, the following transfer functions are used:

$$G_1(s) = \frac{\phi(s)}{\delta(s)}, \quad G_2(s) = \frac{\psi(s)}{\delta(s)} \tag{1}$$

Where, ϕ is the roll angle, ψ is the yaw or heading angle and δ is the rudder angle. The main features of these transfer functions are that G_1 is NMP and presents a resonant peak around the natural frequency of the ship, while G_2 has a pure

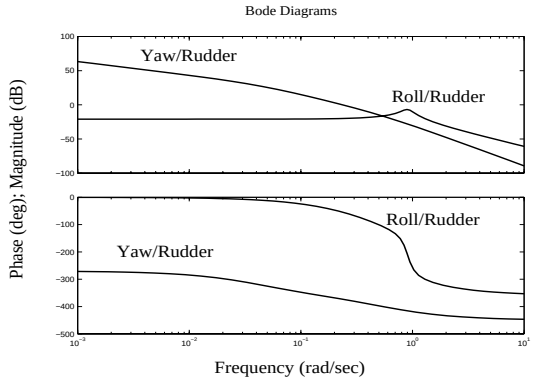

Figure 1: Open loop transfer functions

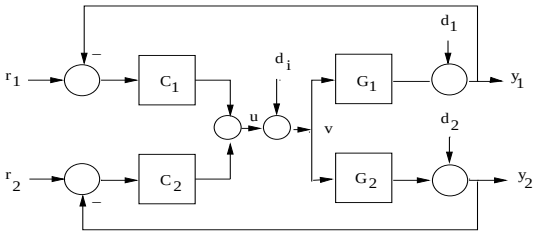

Figure 2: Control Scheme for RRS

integrator. Figure 1 shows these characteristics for the ship data given in the appendix.

3 Control Objectives and Constraints

The control problem can be described using the block diagram given in figure 2, where: y_1 is the Roll angle; y_2 is the Yaw angle; r_1 and r_2 are the Roll and Yaw setpoints, which are taken as 0; d_1 is the wave-produced Roll disturbance; d_2 is the wave-produced Yaw disturbance; and d_i is an input representing unmodelled rudder dynamics. C_1 is the Roll controller and C_2 is the Yaw controller.

Let the multivariable transfer function matrices $G(s)$ and $C(s)$ be defined as follows

$$G(s) \triangleq \begin{bmatrix} G_1(s) \\ G_2(s) \end{bmatrix}, \quad C(s) \triangleq \begin{bmatrix} C_1(s) & C_2(s) \end{bmatrix} \tag{2}$$

Then the feedback system given in figure 2 is described in terms of the following transfer functions: The output open loop transfer function:

$$L_O \triangleq G(s)\, C(S) \tag{3}$$

The output sensitivity and complementary sensitivity functions:

$$S_O \triangleq (I + L_O)^{-1} \quad T_O \triangleq L_O(I + L_O)^{-1} \tag{4}$$

These transfer functions inter-relate the signals in the block diagram given in figure 2 as follows:

$$Y(s) = S_o(s)D_o(s) + S_o(s)G(s)D_i(s) + T_o(s)R(s) \tag{5}$$

Where

$$Y(s) \triangleq \begin{bmatrix} y_1(s) \\ y_2(s) \end{bmatrix} \; D_o(s) \triangleq \begin{bmatrix} d_1(s) \\ d_2(s) \end{bmatrix} \; R(s) \triangleq \begin{bmatrix} r_1(s) \\ r_2(s) \end{bmatrix} \tag{6}$$

The objectives to be achieved by the RRS are: *increase the roll damping, reduce the roll amplitude and control the heading of the ship.*

According to these control objectives, from (5) it follows that the output sensitivity function needs to be reduced at the frequencies of interest so as to attenuate the effect on roll of the wave-produced disturbance $D_o(s)$. The capacity to do this, however, it is expected to be limited by the NMP zero of $G_1(s)$.

4 Limitations due to the NMP zero in RRS

It is well known that NMP zeros affect the achievable performance of a system. This limitations can be described using integrals in the frequency domain. In this section, these integral constraints are reviewed, and the associated design limitations are interpreted.

4.1 Review of Poisson Integral Formula

It is worth noting that The NMP zero in $G_1(s)$ is not a transmission zero of $G(s)$, thus this zero will only affect the roll sensitivity performance. This means that the cost imposed by this NMP zero cannot be shared by the yaw sensitivity. Therefore the constraint reduces to a SISO case [8].

From figure 2, the sensitivity of the roll loop is given by:

$$S_{11}(s) = \frac{1 + C_2(s)G_2(s)}{1 + C_2(s)G_2(s) + C_1(s)G_1(s)}$$

For the NMP zero $q = \sigma_q + j\omega_q$ of $G_1(s)$, $S_{11}(q) = 1$, and assuming closed loop stability the following integral constraint holds [8]:

$$\int_{-\infty}^{\infty} \log|S_{11}(j\omega)| \, \frac{\sigma_q}{\sigma_q^2 + (\omega_q - \omega)^2} d\omega \geq 0 \tag{7}$$

4.2 Design Interpretations

The weighting function in (7), is called the Poisson kernel for the right half plane, and takes explicit account of the effect of the additional phase lag introduced by an ORHP zero $\sigma_q + j\omega_q$. To see this, given an interval $[\omega_1, \omega_2]$ with $\omega_2 > \omega_1 > 0$, consider the integral of the weighting function, *i.e.*,

$$\begin{aligned} \Theta_{s_q}(\omega_1, \omega_2) &\triangleq \int_{\omega_1}^{\omega_2} \frac{\sigma_q}{\sigma_q^2 + (\omega_q - \omega)^2} \, d\omega \\ &= \arctan \frac{\omega_2 - \omega_q}{\sigma_q} - \arctan \frac{\omega_1 - \omega_q}{\sigma_q} \end{aligned} \tag{8}$$

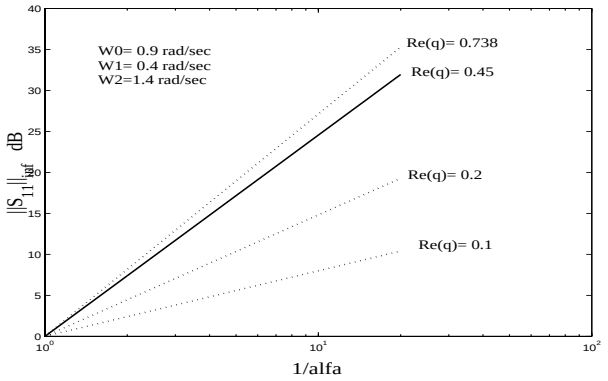

Figure 3: Sensitivity trade-off due to the NMP zero.

This is a frequency weighted interval.

Now, suppose that the feedback loop has been designed to achieve

$$|S_{11}(j\omega)| \leq \alpha_1 < 1\ , \qquad \forall \omega \in \Omega_1 \triangleq [\omega_1, \omega_2] \tag{9}$$

Then the infinity norm of the sensitivity function S_{11} has a lower bound:

$$\|S_{11}\|_\infty \geq \left(\frac{1}{\alpha_1}\right)^{\frac{\Theta_q(\omega_1,\omega_2)}{\pi - \Theta_q(\omega_1,\omega_2)}} \tag{10}$$

Dividing the range of integration in (7), using the inequality (9) and the fact that $|S_{11}(j\omega)| \leq \|S_{11}\|_\infty, \forall \omega$, the following holds:

$$\log \alpha_1\ \Theta_q(\omega_1, \omega_2) + \log \|S_{11}\|_\infty\ [\pi - \Theta_q(\omega_1, \omega_2)] \geq 0.$$

The result (10) is obtained by exponentiating both sides of the last expression.

It is immediate from (10) that the lower bound on the sensitivity peak is strictly greater than one. Indeed, this follows from the fact that $\alpha_1 < 1$ and $\Theta_q(\omega_1, \omega_2) < \pi$. Furthermore, the more the sensitivity is pushed down, *i.e.*, the lower is α_1, and the bigger is the interval $[\omega_1, \omega_2]$, then the bigger will be the peak at frequencies outside that interval. Another, important fact is that given ω_1 and ω_2, expression (10) can be used to analyze the worst location of the NMP zero relative to the interval $[\omega_1, \omega_2]$, *i.e.*, the location of the zero that would bring the highest lower bound on $\|S_{11}\|_\infty$. This occurs at $\sigma_q = \sqrt{\omega_1\ \omega_2}$.

As an illustration of the constraint, consider the data given in the appendix. For this vessel, the natural roll frequency is $\omega_0 = 0.9$ rad/sec, and the range of sensitivity reduction considered is $\omega_1 = 0.4$ rad/sec and $\omega_2 = 1.4$ rad/sec and the NMP is located at $q = 0.45$. Figure 3 shows a graphic representation of the trade-off sensitivity reduction and sensitivity peak for this vessel. This figure also shows cases for different hypothetical positions of the NMP zero. For robustness purposes and high frequency noise rejection it is usually necessary to constraint T_{11}. Thus, let us assume that the following constraint is also imposed:

$$|T_{11}(j\omega)| \leq \alpha_3 < 1 \tag{11}$$

for all $\omega \in \Omega_2 \triangleq [-\infty, -\omega_3] \cup [\omega_3, \infty]$. Note that (11) implies $|S_{11}(j\omega)| \leq 1 + \alpha_2$, $\forall \omega \in \Omega_3$. Then, using this additional information, the following expression is obtained:

$$\begin{aligned} \|S_{11}\|_\infty \geq & \left(\frac{1}{\alpha_1}\right)^{\frac{\Gamma_q(\omega_2) - \Gamma_q(\omega_1)}{\Gamma_q(\omega_3) + \Gamma_q(\omega_1) - \Gamma_q(\omega_2)}} \\ & \times \left(\frac{1}{1+\alpha_2}\right)^{\frac{\pi - \Gamma_q(\omega_3)}{\Gamma_q(\omega_3) + \Gamma_q(\omega_1) - \Gamma_q(\omega_2)}} \end{aligned} \tag{12}$$

Where, $\Gamma(\omega_i) \triangleq \arctan \frac{\omega_i - \omega_q}{\sigma_q}$, for $i = 1, 2, 3$. From this last expression it is clear that the lower the bandwith of T_{11} and the smaller α_2, the bigger will be the contribution to the lower bound on $\|S_{11}\|_\infty$. However, If $\omega_3 \gg \omega_2$ (12) reduces to (10). A similar expression to (12) is given in [4]. Indeed, (12) justifies the fact the that the peak of the roll sensitivity function will occur close to the zone of sensitivity reduction, if ω_3 is close to ω_2 as was assumed in [4].

The above analysis has shown the implications of the NMP zero on the roll closed loop performance. Note that the results hold for any controller as long as it ensures closed loop stability. In the next section the issues related to the SITO nature of the problem are analyzed.

5 Trade-off Between Roll Reduction and Yaw Interference

The trade-off between Roll reduction and Yaw interference is investigated next. First some background concepts are presented.

5.1 Wave Disturbance Model

The wave disturbances act over the entire hull [3]. As a result, the disturbances are considered at the output as its shown in figure 2. These disturbances can be characterized in terms of their frequency spectrum, for instance, using the Pierson-Moskowits spectrum, see [1]. This frequency spectrum can be simulated by either a series of added sinusoidal signals, or using filtered white noise. In the latter case, the filter used to approximate the spectrum is of the form

$$F(s) = \frac{K_w\ s}{s^2 + 2\ \xi\ \omega_e\ s + \omega_e^2} \tag{13}$$

in which K_w is a constant describing the wave intensity, ξ is a damping coefficient, and ω_e is the encounter frequency, which depends on the dominate wave frequency, the forward speed of the ship, and the angle between the heading and the direction of the waves. For more detail see [1].

If the white noise driving the filter has a power spectral density σ_n^2 then the power spectral density of the disturbance is

given by

$$S_d(j\omega) = |F(j\omega)|^2 \sigma_n^2 \tag{14}$$

5.2 Controller Parameterization and Internal Stability

For a stable plant $G(s)$ all controllers $C(s)$ yielding an internal stable closed loop can be parameterized as:

$$C(s) = [I - Q(s)G(s)]^{-1} Q(s) \tag{15}$$

where $Q(s)$ belongs to the set of all matrices with appropriate dimensions which are stable, proper, and having real-rational functions entries, see Vidyasagar [9].

If the plant $G(s)$ is not stable (as is the case for the ship due to the existence of pure integrator in $G_2(s)$), (15) still holds. However, $Q(s)$ must satisfy further interpolation constraints. Using the parametrization (15), it follows that the system is internally stable provided the following four transfer function matrices are stable:

$$\begin{bmatrix} [I - G(s)Q(s)] & -G(s)[I - Q(s)G(s)] \\ Q(s) & [I - Q(s)G(s)] \end{bmatrix} \tag{16}$$

For the SITO case, $Q(s)$ is of the form $Q(s) = [Q_1(s)\ Q_2(s)]$. Taking into account the fact that $G_2(s)$ has a pole at the origin, and using (16), then it follows that interpolation constraints that must be satisfied to ensure internal stability in this case are:

- $Q_1(s)$ and $Q_2(s)$ should be stable.
- $Q_1(0) = 0$ and $Q_2(0) = 0$.
- $G_2(0)\ Q_2(0) = 1$

5.3 Roll Reduction and Yaw Interference Cost Function

In order to analyze the trade-off between Roll Reduction and Yaw Interference imposed by the single input two output nature of the system, it will be assumed that the roll disturbance is the only disturbance present, *i.e.*, only d_1 is considered in figure 2. This is a realistic assumption since the impact of wave on Yaw is relatively weak in open loop. As a consequence of this assumption, and null setpoints, the two outputs are given by:

$$Y_1(s) = (1 - G_1(s)Q_1(s))D_1(s) \tag{17}$$

$$Y_2(s) = G_2(s)Q_1(s)D_1(s) \tag{18}$$

while the corresponding power spectral densities are given by:

$$S_{y_1}(j\omega) = |1 - G_1(j\omega)Q_1(j\omega)|^2 S_d(j\omega) \tag{19}$$

$$S_{y_2}(j\omega) = |G_2(j\omega)Q_1(j\omega)|^2 S_d(j\omega) \tag{20}$$

For the signals $y_1(t)$ and $y_2(t)$ define the autocorrelation functions

$$R_{y_i}(\tau) \triangleq \lim_{T\to\infty} \frac{1}{2T} \int_{-T}^{+T} y_i(t) y_i(t+\tau)\, dt \quad for\ i = 1, 2. \tag{21}$$

These autocorrelation functions are the inverse Fourier transform of the power spectral densities $S_{y_1}(j\omega)$ and $S_{y_2}(j\omega)$. Besides, the autocorrelation functions evaluated at zero give the corresponding square average power of the signals. Thus,

$$\overline{pow}^2(y_i) = \frac{1}{2\pi} \int_{-\infty}^{+\infty} S_{Yi}(j\omega) d\omega \quad for\ i = 1, 2. \tag{22}$$

These integrals can be used to define a cost function that reflects the relative importance of each output. Therefore, the following ***Roll Reduction and Yaw Interference Cost Function*** is defined:

$$\begin{aligned} J \triangleq \lambda \int_{-\infty}^{+\infty} |1 - G_1(j\omega)Q_1(j\omega)|^2 S_d(j\omega)\, d\omega \\ +(1-\lambda) \int_{-\infty}^{+\infty} |G_2(j\omega)Q_1(j\omega)|^2 S_d(j\omega)\, d\omega \end{aligned} \tag{23}$$

or in a more compact form

$$J = \lambda J_{Roll} + (1 - \lambda) J_{Yaw} \tag{24}$$

Where $\lambda \in [0\ 1]$ is a scalar that weights the importance of Roll reduction with respect to Yaw interference. Thus, $\lambda = 1$ ensures that all the effort of the control is aimed at minimizing roll power without caring about Yaw interference. Similarly, $\lambda = 0$ ensures that all the effort of the control is aimed at keeping the course without caring about Roll.

The optimization problem is thus to find the optimal controller factorization $Q^{opt}(s)$ subject to the interpolation constraints given in subsection 5.2 that minimizes the function defined by (23), given λ and the power spectral density of the wave disturbances. Note that this is a SITO cheap control problem since rudder effort is not being penalized. Hence, the solution will give a benchmark against which practical designs can be compared. This is consistent with the use of cheap control as a benchmark in single input single output (SISO) control problems.

5.4 Quadratic Optimal Q synthesis

In this subsection, the solution of the optimization problem proposed in the previous subsection is given.

Using expression (14), the function defined in (23), can be expressed as

$$\begin{aligned} J = \lambda \sigma_n^2 \int_{-\infty}^{+\infty} |F(j\omega) - G_1(j\omega)Q_1(j\omega)F(j\omega)|^2\, d\omega \\ +(1-\lambda)\sigma_n^2 \int_{-\infty}^{+\infty} |G_2(j\omega)Q_1(j\omega)F(j\omega)|^2\, d\omega \end{aligned} \tag{25}$$

Since $Q_1(0) = 0$ is necessary to ensure stability, then $Q_1(j\omega)$ is factored as follows:

$$Q_1(j\omega) \triangleq (j\omega)\widetilde{Q}_1(j\omega), \tag{26}$$

To simplify the development, the following quantities are defined:

$$L(j\omega) \triangleq \sigma_n\sqrt{\lambda}F(j\omega) \tag{27}$$

$$D(j\omega) \triangleq \sigma_n\sqrt{\lambda}(j\omega)G_1(j\omega)F(j\omega) \tag{28}$$

$$E(j\omega) \triangleq \sigma_n\sqrt{1-\lambda}(j\omega)G_2(j\omega)F(j\omega) \tag{29}$$

Using (26), (27), (28) and (29), in (25) the cost function can be manipulated into the form:

$$J = \overline{J} + \int_{-\infty}^{+\infty} |W(j\omega) - V(j\omega)\widetilde{Q}_1(j\omega)|^2 \, d\omega \tag{30}$$

where $\overline{J}$ is independent of $\widetilde{Q}_1(j\omega)$, and $V(j\omega)$ is given by the following spectral factorization:

$$\begin{aligned} |V(j\omega)|^2 = V(-j\omega)V(j\omega) &\triangleq |D(j\omega)|^2 + |E(j\omega)|^2 \\ &= D(-j\omega)D(j\omega) + E(-j\omega)E(j\omega), \end{aligned} \tag{31}$$

and

$$W(j\omega) \triangleq \frac{V(j\omega)L(j\omega)D(j\omega)}{|V(j\omega)|^2} \tag{32}$$

Finally, introducing the notation $\|\cdot\|_2$, for (30), then the optimization problem takes the general form

$$\widetilde{Q}_1^{opt}(j\omega) = \arg \min_{\widetilde{Q}_1(j\omega)\in\mathcal{S}} \|W(j\omega) - V(j\omega)\widetilde{Q}_1(j\omega)\|_2^2 \tag{33}$$

where $\mathcal{S}$ is the ring of all proper stable transfer functions. The solution of the above problem is given by the following theorem.

Theorem 5.1. *Suppose that $W(j\omega)$, $\widetilde{Q}_1(j\omega)$ and $V(j\omega) \in \mathcal{S}$ and that $V(j\omega)$ has the form $V(j\omega) = D_v(j\omega)V_1(j\omega)$, where $V_1(j\omega) \in \mathcal{S}$ has no zeros at all points on the $j\omega$-axis and at infinity, while $D_v(j\omega) \in \mathcal{S}$ where the only $\mathbb{C}_{+e}$ -zeros [1] (if any) are at infinity or on the $j\omega$-axis. Under this conditions,*

$$\begin{aligned} &\inf_{\widetilde{Q}_1(j\omega)\in\mathcal{S}} \|W(j\omega) - V(j\omega)\widetilde{Q}_1(j\omega)\|_2 \\ &= \inf_{\widetilde{Q}_1(j\omega)\in\mathcal{S}} \|W(j\omega) - V_1(j\omega)\widetilde{Q}_1(j\omega)\|_2 \end{aligned} \tag{34}$$

and

$$\begin{aligned} &\arg \min_{\widetilde{Q}_1(j\omega)\in\mathcal{S}} \|W(j\omega) - V_1(j\omega)\widetilde{Q}_1(j\omega)\|_2^2 \\ &= (V_{1m}(j\omega))^{-1}[V_{1a}(j\omega)^{-1}W(j\omega)]_s \end{aligned} \tag{35}$$

[1] $\mathbb{C}_{+e}$ denotes the extended CRHP, *i.e.*, the CRHP together with the point at infinity.

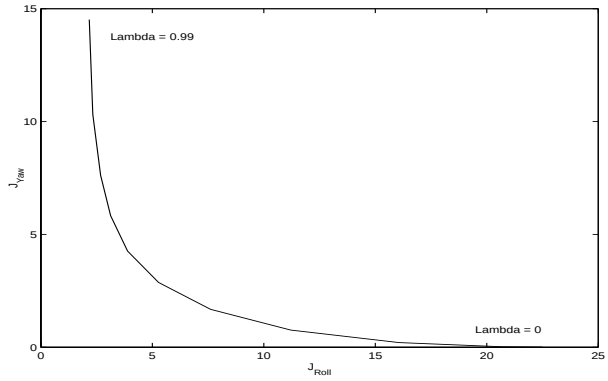

Figure 4: Graphic Representation of the Roll reduction vs. Yaw interference trade-off.

where

$$V_1(j\omega) = V_{1m}(j\omega)V_{1a}(j\omega) \tag{36}$$

such that $V_{1m}(j\omega)$ is a factor with poles and zeros in the LHP, and $V_{1a}(j\omega)$ is an all pass factor with unitary gain, and where $[X]_s$ denotes the stable part of X.

Proof: This follows from Lemma 10 in [9] pp.171-172, and Lemma 16.2 in [10] pp.458-459. □

5.5 Roll Reduction vs. Yaw Interference

Once $\widetilde{Q}_1^{opt}(j\omega)$ has been found as a function of λ, then the cost function (24) can be evaluated using the residue theorem. Then a plot of J_{Yaw} vs. J_{Roll} using λ as a parameter can be made, see figure 4. This plot is a graphical representation of the trade-off inherit in Roll-Yaw interaction in this SITO problem. Figure 4 corresponds to the numerical data given in appendix. The first characteristic to observe from figure 4 is that the Roll cost cannot be reduced to zero. This is a predictable result since with $\lambda = 1$ the optimization problem reduces to a SISO cheap control problem with a NMP zero, and this NMP zero imposes a lower limit on the achievable cost, see [11], [7]. It is also predictable that, as the spectrum of the wave disturbance moves past the NMP zero the lower limit of the cost will increase. This, again, evidences the relationship between the location of the NMP zero and the range of frequencies in which disturbance rejection is desired (see section 4.2).

The key novel feature presented here, is the characterization of the interaction between the reduction of average power of the two outputs due to the SITO nature of the plant. Indeed figure 4 represents a fundamental SITO trade-off since it shows the *price paid* for reducing the roll (average power) in terms of the increased Yaw angle (average power).

Finally, if the control strategy is concerned with keeping the heading only, from figure 4 it is evident that the cost can be reduced to zero. This is in agreement with the results of section 4.2 as the NMP has no effect on the heading.

6 Conclusions

This paper has analyzed fundamental limitations imposed on the achievable closed loop performance by the non minimum phase and SITO characteristics of the rudder roll problem.

It was found that the NMP zero only affects the roll performance, and that an attempt to design a controller that forces the roll sensitivity to be small in a range of frequencies near the NMP zero will result in high sensitivity in other frequency ranges. Formulas to quantify the trade off are given.

In regards the SITO nature of the problem, there is trade-off between Roll reduction and Yaw interference. This trade-off has been characterized using a cheap control cost function that relates the average power of the Roll and Yaw angles. Thus, any control strategy can be compared against this result.

A Ship Model and Wave disturbance Data

In this appendix, the rudder to Roll and Yaw transfer functions for a constant forward speed of a naval vessel of 9 m/sec are given. The Ship parameters of the model were taken from Blanke and Christensen [3].

$$G_1 = \frac{\phi(s)}{\delta_c(s)} = \frac{-0.0894s + 0.0404}{s^3 + 0.7595s^2 + 0.9331s + 0.4515}$$

$$G_2(s) = \frac{\psi(s)}{\delta_c(s)} = \frac{-0.0334}{s(s^2 + 0.5966s + 0.0231)}$$

The power spectral density of the noise is $\sigma_n^2 = 1$, and the disturbance filter is given by

$$F(s) = \frac{s}{s^2 + 2\,(0.1)\,(0.5)\,s + (0.5)^2}$$

References

[1] Fossen Thor, *Guidance and Control of Ocean Vehicles*. John Wiley and Sons Ltd. 1994.

[2] van Amerongen J., van der Klugt P., and van Nauta Lemke H., Rudder Roll Stabilization for Ships. *Automatica*, VOl. 26, No. 2, pp.679-690. 1990.

[3] Blanke M. and Christensen A., Rudder-Roll Damping Autopilot Robustness to Sway-Yaw-Roll Couplings, SCSS, Proceedings, 10th SCSS, Ottawa, Canada. 1993.

[4] Hearns G. and Blanke M., Quantitative Analisis and Design of a Rudder Roll Damping Controller, IFAC CAMS1998. 1998.

[5] Perez T., Tzeng C-Y, and Goodwin G.C., Model Predictive Rudder-Roll Stabilization Control for Ships, to appear in the 5th IFAC MCMC2000, Denmark. 2000.

[6] Roberts G. N., A Note on the Applicability of RudderRoll Stabilisation for Ships, Proceedings of the American Control Conference, San Francisco, California, U.S.A. 1993.

[7] Qiu L. and Davison E. J., Performance Limitations of Non Minimum Phase Systems in the Servomechanism problem. Automatica,29(2), pp. 337-349. 1993.

[8] Seron M.M., Braslavsky J., and Goodwin G.C. *Fundamental Limitations in Filtering and Control*, Springer. 1993.

[9] Vidyasagar M., *Control System Synthesis: A Factorization Approach*, The Massachusetts institute of Technology. 1985.

[10] Goodwin G, Graebe S. and Salgado M., *Control System Design*, Prentice-Hall. 2000.

[11] Kwakernaak H. and Sivan R., *Linear Optimal Control Systems*, John Wiley and Sons Inc. 1972.